ISSN 1062-8738, Bulletin of the Russian Academy of Sciences: Physics, 2025, Vol. 89, No. 7, pp. 1086–1092. © Pleiades Publishing, Ltd., 2025.

Dynamics of a Chain of Interacting Magnetic Particles in a One-Dimensional Periodic Energy Landscape

M. N. Kourov[a], A. E. Samoilova[a, b, c, *], and A. V. Straube[d, **]

[a] *Perm State University, Perm, 614068 Russia*

[b] *Institute of Continuous Media Mechanics, Ural Branch, Russian Academy of Science, Perm, 614013 Russia*

[c] *Lobachevsky State University of Nizhny Novgorod, Nizhny Novgorod, 603022 Russia*

[d] *Zuse Institute Berlin, Berlin, 14195 Germany*

**e-mail: annsomeoil@gmail.com*

***e-mail: straube@zib.de*

Received December 13, 2024; revised March 17, 2025; accepted March 31, 2025

Abstract—We explore the dynamics of a one-dimensional chain of paramagnetic colloidal particles in a periodic potential. The model accounts for a constant external force, along with magnetic dipolar attraction and hard-core repulsive interactions between particles. Numerical simulations reveal the emergence of a traveling kink – a chain defect propagating along the chain. We show that the kink emerges beyond a critical force threshold and identify parameter regimes corresponding to distinct dynamic modes such as a pinned kink, a running kink, a cluster kink, and chain drift.

Keywords: colloidal particles, chain of interacting particles, periodic potential, traveling kink, soliton

DOI: 10.1134/S1062873825711742

INTRODUCTION

Studying the dynamics of interacting particles in confined (or constrained) geometries is a central problem that arises across various fields of science and technology [1]. A striking example in medical applications is the need for targeted delivery of active agents or drugs to a prescribed location [2]. This issue is also relevant in the context of the fundamental problem of friction: when two surfaces slide relative to one another, the interaction of their microscopic surface irregularities (i.e., roughness) determines macroscopic friction [3]. A similar problem can arise when interacting colloidal particles slide over a nonuniform landscape [4].

Colloidal particles, capable of moving through different geometric or energetic landscapes under the influence of external forces, represent a broad class of intensively studied systems. In the stationary state, each particle tends to occupy a position corresponding to a potential minimum. When the number of particles exceeds the number of minima, some particles are left without enough free space. They squeeze between other particles and displace their neighbors to create sufficient space (see Fig. 1a), leading to the formation of defects. The application of an external force can set these defects in motion (see Fig. 1b). Additionally, various interactions between particles can influence the dynamics of such defects. The localized structure (defect) that propagates through the system is typically referred to as a soliton or a running kink.

In colloidal systems, similar structures were first observed in an experiment involving a two-dimensional potential, where the emergence of both kinks (compactions) and anti-kinks (vacancies) was demonstrated [5]. The appearance of a kink along a linear array of particles was also observed experimentally in a similar quasi-one-dimensional system [6]. Additionally, we note the ring geometry, in which similar structures—referred to as solitons—have recently been predicted theoretically [7] and observed experimentally [8].

In the present study, we focus on a chain of finite-size colloidal particles placed in a one-dimensional periodic potential. We will assume that a constant external force acts on the system, and that the particles possess paramagnetic properties, allowing them to interact with each other through dipole-dipole interactions. The aim of this work is to construct a simple theoretical model that enables the emergence of a kink, and to analyze other discrete structures that can arise in this system.

MODEL OF COLLOIDAL PARTICLE DYNAMICS

Consider colloidal particles of spherical shape suspended in a viscous liquid. By colloidal particles, we

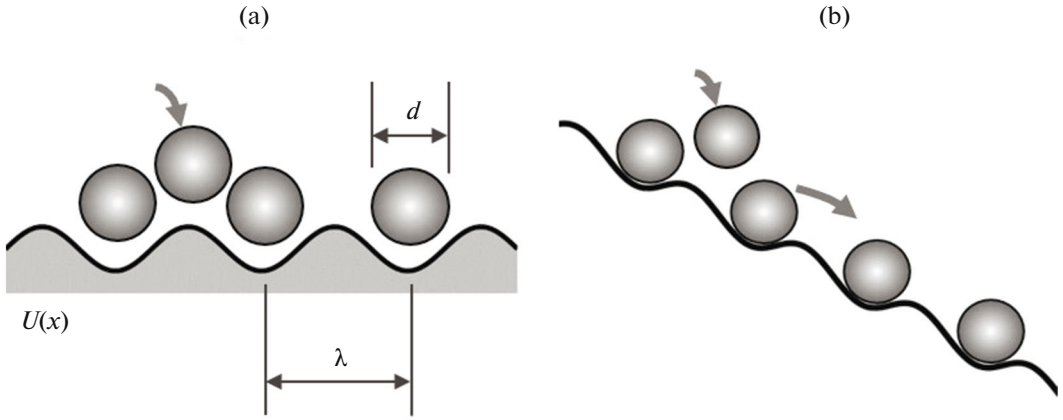

Fig. 1. One-dimensional chain of particles with diameter d in a periodic landscape of spatial period λ: defect formation due to an "extra" particle (a); kink excitation in the presence of an external force f_E (landscape tilt) (b).

refer to particles with sizes ranging from hundreds of nanometers to several micrometers. For example, in the experiments [6, 9], magnetic particles with a diameter of 3 μm were used. In the one-dimensional case, the behavior of each individual particle, with coordinate $x(t)$, is governed by the following equation neglecting inertia:

$$\zeta \frac{dx(t)}{dt} = F(x,t), \tag{1}$$

where ζ is the viscous friction coefficient, which, in the Stokes approximation, has the form $\zeta = 6\pi\eta a$ (here, η is the dynamic viscosity of the fluid and a is the radius of the particle). On the right-hand side in $F(x,t)$, we include all forces acting on the particle, except for friction: both external forces and interparticle interaction forces. We restrict ourselves to building a minimal model, neglecting thermal fluctuations.

Let us account for the external forces acting on the particle. As mentioned above, a periodic energy landscape can be created using a linear array of optical tweezers placed at equal distances [6, 9]. Each optical tweezer individually induces a potential well with a Gaussian profile [9, 10]. When the traps are arranged closely enough to allow partial overlap of neighboring potential wells, the resulting superposition of the optical tweezer array is well approximated by a harmonic potential [9] (see also Fig. 1a):

$$U_T(x) = U_L(1 - \cos kx), \tag{2}$$

where the amplitude U_L is determined by the characteristics of the optical tweezers, $k = 2\pi/\lambda$ is the wave number, and the spatial period λ defines the distance between the centers of the potential wells. The force exerted on the particle by the landscape is given by:

$$F_T(x) = -\frac{dU_T(x)}{dx} = -f_L \sin(kx). \tag{3}$$

For convenience, we introduce the notation $f_L = U_L k$ for the amplitude of the force characterizing the periodic landscape. The introduction of a constant external force f_E, acting perpendicular to the humps of the optical landscape, is equivalent to adding a potential term $-f_E x$. In this case, the magnitude of f_E determines the tilt of the landscape, breaking its spatial symmetry. Thus, in the presence of an external force, the energy landscape along which the particles move is defined by the full potential (Fig. 1b):

$$U(x) = \frac{f_L}{k}(1 - \cos kx) - f_E x. \tag{4}$$

A similar situation arises in a system with a magnetic substrate [11].

Without interparticle interactions, the equation of motion of a colloidal particle (1) in a potential from Eq. (4) takes the form:

$$\zeta \frac{dx}{dt} = f_E - f_L \sin kx, \tag{5}$$

where the force is given by $F(x) = -dU(x)/dt = F_T(x) + f_E$.

By passing to dimensionless coordinate and time variables, $\tilde{x} = x/\lambda$, $\tilde{t} = tf_L/(\lambda\zeta)$, the equation of motion (5) transforms into the well-known Adler equation [12]:

$$\frac{d\tilde{x}}{d\tilde{t}} = f - \sin(2\pi\tilde{x}), \tag{6}$$

where $f = f_E/f_L$ is the dimensionless external force. For brevity, the tilde "~" notation for dimensionless variables will be omitted in the following.

The dynamics of the particle are clearly determined by the ratio of the forces characterizing the landscape amplitude and the external influence, f_L and f_E. The particle becomes "stuck" in the potential well when

$f < 1$ ($f_E < f_L$). In this case, the particle's position reaches a limit value:

$$x_0 = \frac{1}{2\pi}\arcsin f \pmod 1, \quad f < 1, \tag{7}$$

which is a stationary solution of Eq. (6). In the opposite case, $f > 1$ ($f_E > f_L$), no equilibrium exists, and the particle continuously slides down along the landscape with a velocity $V(t)$. The particle's drift velocity $\langle V\rangle$ is obtained by time-averaging $V(t)$ and exhibits a square-root dependence on the external force [9]:

$$\langle V\rangle = \sqrt{f^2 - 1}, \quad f \geq 1. \tag{8}$$

To simplify the analysis of defect dynamics, we assume that before introducing an "extra" particle, each local minimum of the potential is occupied by exactly one particle. In the absence of interactions, such an initial configuration should remain stationary. Therefore, in the following, we will primarily focus on the case $f < 1$.

Next, we account for interactions that may arise in a chain of particles with paramagnetic properties. We assume that these particles are weakly magnetized in an external magnetic field, so that each particle possesses an instantaneously induced magnetic moment [13] (in the more general case, the relaxation time is finite [14]):

$$\vec{m} = V\chi_{\text{eff}}\vec{H}, \tag{9}$$

where V is the volume of the particle, χ_{eff} is the effective magnetic susceptibility, and $\vec{H}$ is the external magnetic field. The interaction between a pair of particles with magnetic moments $\vec{m}_1$ and $\vec{m}_2$ is determined by the energy of the dipole-dipole (superscript "dd") interaction [15]:

$$U^{\text{dd}}(r_{12}) = \frac{\mu_0}{4\pi r_{12}^3}\left(\vec{m}_1\cdot\vec{m}_2 - 3(\vec{m}_1\cdot\hat{\vec{r}}_{12})(\vec{m}_2\cdot\hat{\vec{r}}_{12})\right), \tag{10}$$

where μ_0 is the magnetic permeability of vacuum, $\vec{r}_{12} = \vec{r}_1 - \vec{r}_2$ is the vector connecting the centers of the particles, $\hat{\vec{r}}_{12} = \vec{r}_{12}/r_{12}$ is the corresponding unit vector, and $r_{12} = |\vec{r}_{12}|$ is the distance between the particles. In the case of identical dipoles, $\vec{m}_1 = \vec{m}_2 = \vec{m}$, the expression for the potential energy (11) simplifies significantly:

$$U^{\text{dd}}(r_{12}) = \frac{\mu_0 m^2}{4\pi r_{12}^3}\left(1 - 3\cos^2\vartheta\right), \tag{11}$$

where ϑ is the angle between the magnetic field and the axis connecting the particles. It is known that the critical angle $\vartheta_c = 54.7°$ marks the boundary between regions of attractive and repulsive interactions. For $\vartheta > \vartheta_c$, particle repulsion occurs, while for $\vartheta < \vartheta_c$, particle attraction takes place. When the field is oriented along a linear sequence of particles [6] $\vec{H} = H\hat{e}_x$ ($\vartheta = 0$), the interaction potential is purely attractive:

$$U^{\text{dd}}(r_{12}) = -\frac{\mu_0(V\chi_{\text{eff}}H)^2}{2\pi}\frac{1}{r_{12}^3}, \tag{12}$$

which contributes to the formation of chains [16]. Measuring the forces in units of f_L, the dimensionless dipole-dipole interaction force exerted by particle j on particle i, corresponding to expression (12), reads:

$$f_{ij}^{\text{dd}} = -\frac{\partial}{\partial x_i}U^{\text{dd}}(r_{ij}) = -C\frac{(x_i - x_j)}{r_{ij}^5}, \tag{13}$$

where x_i and x_j are the coordinates of the ith and jth particles, respectively, and $r_{ij} = |x_i - x_j|$ is the distance between them. Here, C is a dimensionless parameter characterizing the strength of this interaction. A value of zero disables the dipole-dipole interaction.

There are also short-range repulsive forces between the particles in the chain. These forces act at very short distances and arise because the particles have a finite size and cannot overlap. Depending on the specific numerical implementations, various authors apply different smoothing modifications of the hard-sphere model. In this work, we use the following type of repulsive force (denoted by the superscript 'hc' for 'hard core') [17]:

$$f_{ij}^{\text{hc}} = \begin{cases} 96\varepsilon\left[2\left(\dfrac{d}{r_{ij}}\right)^{48} - \left(\dfrac{d}{r_{ij}}\right)^{24}\right]\dfrac{x_i - x_j}{r_{ij}^2}, & r \leq r_0, \\ 0, & r > r_0, \end{cases} \tag{14}$$

where $r_0 = 2^{1/24}d$ is the cutoff distance corresponding to the effective particle diameter, and ε is a dimensionless parameter characterizing the strength of this interaction. This potential is derived from the Lennard-Jones potential [18] (or more rigid modifications of it [19]) by shifting and truncating the attractive tail. To better model the real situation, we use higher powers in the potential (48–24 instead of the standard 12–6), which results in a steeper repulsion.

Taking all these interactions into account, the equation describing the dynamics of N interacting particles in a one-dimensional chain takes the following form:

$$\frac{dx_i}{dt} = f - \sin(2\pi x_i) + \sum_{j\neq i}\left(f_{ij}^{\text{dd}} + f_{ij}^{\text{hc}}\right), \quad i, j \in [1, N]. \tag{15}$$

NUMERICAL METHOD

To model the dynamics of a chain of N particles, we solve a system of first-order differential equations (15). We perform the numerical integration using the Euler

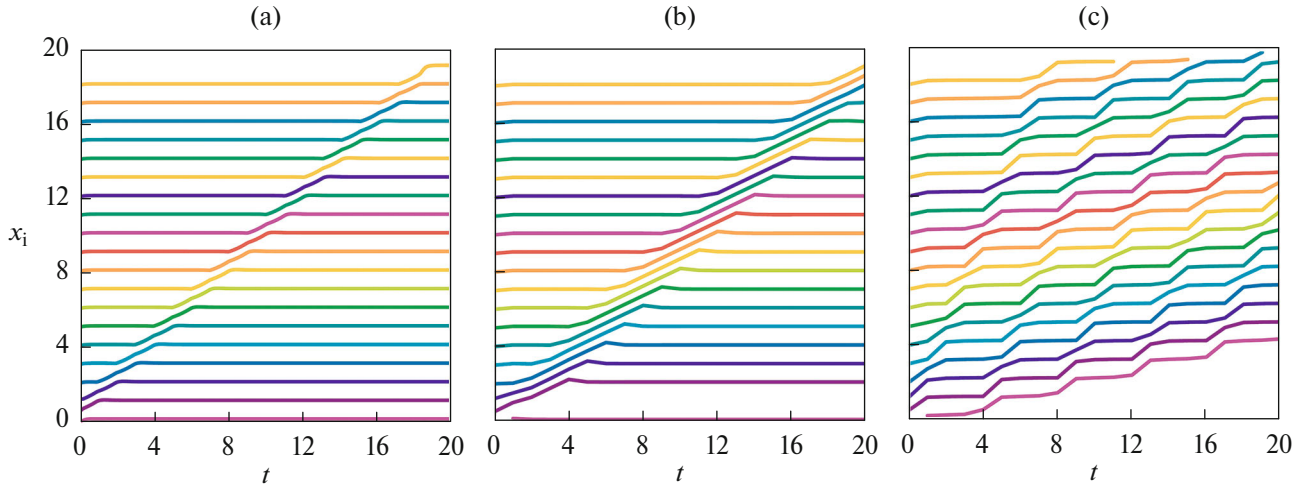

Fig. 2. Coordinates of 20 particles in the chain as a function of time, showing different behaviors of discrete structures: running kink, $C = 0.015, f = 0.5$ (a); clustering, $C = 0.05, f = 0.5$ (b); particle drift, $C = 0.015, f = 1.01$ (c).

method with a time step of 0.001. We carry out the simulations for $N = 9$ and $N = 11$ (tests) and $N = 20$ (main simulations).

In the numerical tests, we initially place the particles equidistantly. For the main simulations, we set up a different initial configuration, placing all particles at equal distances from each other, except for the first three particles. Specifically, we set the coordinates of the particles as $x_i = i$, with the first three particles positioned at –0.2, 0.5, and 1.2, respectively. In this way, we introduce an extra particle into the chain, with each particle initially occupying the local minimum of the potential at $f = 0$, creating a defect near the end of the chain.

In all simulations, we set the diameter of the particles to $d = 0.5$. The values of other dimensionless parameters of the problem—the external force f, the strengths of the dipole-dipole attraction force C, and the short-range repulsion force ε – were varied over a wide range depending on the objectives of the study.

As a test, we analyze the dynamics of a chain of particles with each type of interaction separately. In the first test, we integrate Eqs. (15) for a system of 9 particles, considering only dipole-dipole interactions, without the landscape and short-range repulsion. We show that the particles repel each other more strongly the farther they are from the center of the chain. This behavior occurs because the forces from opposite neighbors are more strongly balanced for the central particles, while they remain almost uncompensated for the particles at the ends of the chain. Such behavior is well known and has been previously observed in a similar one-dimensional system [20].

We perform another test to analyze the realization of short-range interactions that account for the finite particle size. In a system of 11 particles with dipole-dipole attraction and short-range repulsive forces, and without the influence of the landscape, we show that the particles initially attract each other, forming small clusters, which then merge into a single linear cluster of touching particles.

RESULTS AND DISCUSSION

We carry out the main simulations at parameter values $C = 0.015$, $\varepsilon = 0.25$, $f = 0.5$, and values close to them. With these values of interaction and external force parameters, we show that a running kink emerges, closely resembling the structure observed in experiments with a one-dimensional chain of colloidal particles in a periodic landscape [6]. Figure 2a illustrates the time-dependent dynamics of a system of 20 particles under these parameters. The plot reveals a running defect of three particles propagating along the chain. This picture qualitatively reproduces the behavior of the particles in the experiment. However, we emphasize that the perfectly regular nature of the trajectories in Fig. 2a results from the fact that the numerical model neglects the thermal fluctuations that are inevitably present in the experiment.

At distinct values of the parameters, we observe different regimes of the system's behavior. As the external force f or the intensity of interparticle attraction, C, decreases, we detect the kink sticking (or pinning) to the landscape. In this regime, the extra particle introduced at the initial time sticks to its neighbors, and the defect remains completely immobile. That is, the kink stays stationary and fails to propagate, despite the presence of a nonzero external force.

As the parameter C increases, the interaction between the particles becomes so strong that the particles overcome the potential barrier given by the landscape and form clusters. Instead of the motion of a single particle through the system (a single kink), we

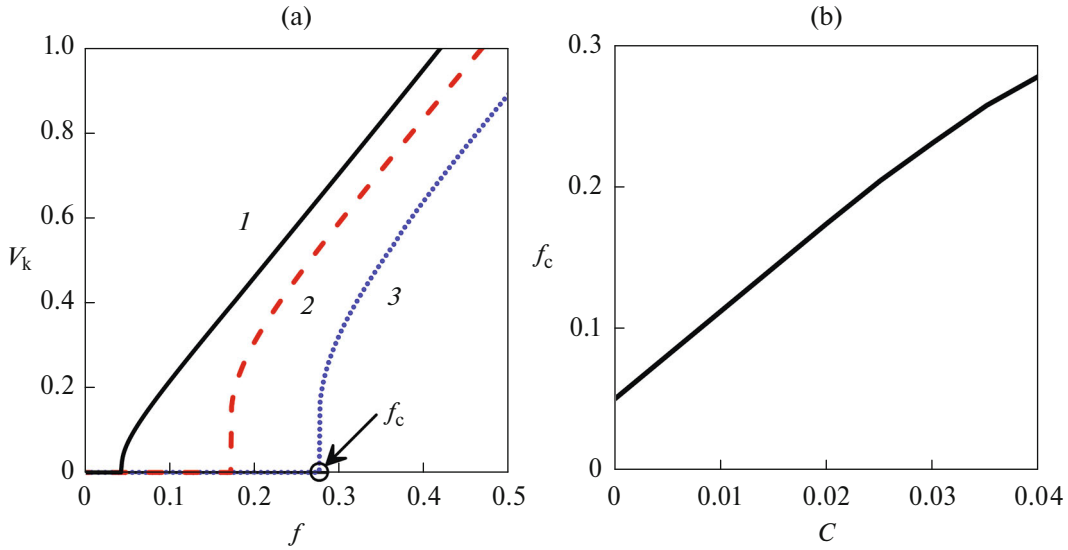

Fig. 3. Dependence of the kink velocity V_k on the external force f at different values of C (a). Curves *1*, *2*, and *3* correspond to $C = 0$, 0.02, 0.04. Dependence of the critical external force f_c on the interaction strength C (b).

observe the motion of a whole cluster of particles (a kink of 2, 3, or 4 particles), as illustrated in Fig. 2b. This behavior resembles the structures observed in ring geometry [7, 8]. However, it is worth emphasizing a significant difference: in contrast to the linear geometry considered here, the ring system lacks long-range interactions.

With a significant increase in the external force f, the system departs from the initial equilibrium state of the chain, where each particle occupies a local minimum of the potential. Thus, when $f > 1$, we observe drift of the entire chain, as illustrated in Fig. 2c.

To clarify the details of the origin of the kink motion, we vary the parameter values between those corresponding to the stationary state and the running kink and compute the average kink velocity V_k. Figure 3a shows plots of the kink velocity dependence on the external force f for different values of the interparticle attraction strength C. As we can see, the kink emerges in a threshold fashion: there is a critical value of the external force f_c at which kink detachment (depinning) occurs. The kink, which remains stationary for $f < f_c$, begins to move beyond $f = f_c$. Afterwards, the kink velocity V_k increases as the external force f is raised. Interestingly, the threshold value, $f_c = f_c(C)$, rises with an increase in dipole-dipole attraction strength C, see Fig. 3b.

Note that the parameter ε has little influence on the dynamics of the chain, as expected from the model approximating the hard-sphere model. The repulsion, which only acts at extremely short distances between particles, is negligible and does not significantly affect the particle dynamics compared to the long-range dipole-dipole attraction. Therefore, in our control simulations, we vary the values of the parameters f and C without altering ε.

We summarize the variety of modes observed in the studied system onto the parameter plane (f, C), see Fig. 4. The map reveals the four types of system dynamics described above: a pinned kink, a running kink, dynamical clustering (a running kink-like structure formed by more than three particles), and drift of the entire chain.

CONCLUSIONS

We have studied the behavior of a one-dimensional chain of paramagnetic particles placed in a periodic potential landscape, under the influence of a constant external force that tilts the landscape. We constructed a model describing the overdamped dynamics of these particles, accounting for the following interparticle interaction forces: long-range dipole-dipole attraction arising from the induced magnetic moments of the particles along the chain, and short-range hard-core repulsion due to the finite size of the particles. The results were obtained by numerically solving the equations over a wide range of control parameters.

In the absence of interactions, the particle dynamics are governed by the Adler equation, which admits an analytical solution. Depending on the strength of the external force, the particles in the chain either occupy a stationary position (i.e., particle pinning or sticking) or drift with an average velocity that follows a square-root-law dependence on the external force. The incorporation of various interactions results in significant changes to the system's dynamics.

The interplay of the periodic potential, external constant force, and interparticle interactions gives rise

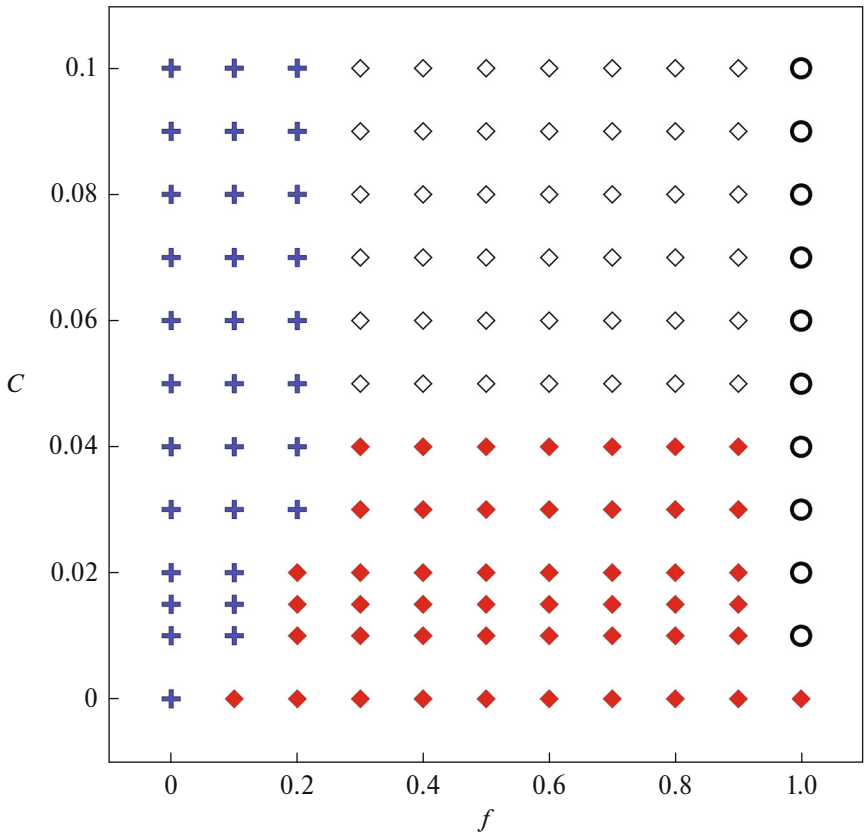

Fig. 4. Map of different modes: (+) stationary (pinned) kink, (♦) running kink, (◇) cluster kink, (○) chain drift.

to intriguing system behavior. At the initial moment, we introduce an extra particle into the chain, where particles are initially positioned at equal distances in the minima of the potential. This setup replicates the conditions of experiments [6], in which the propagation of a localized defect along the chain, known as a running kink, was observed. Our simulations confirm the existence of this structure: at certain parameter values, the chain dynamics qualitatively match the known experimental results.

Apart from the running kink, we also detect other running kink-like cluster structures when the intensity of the dipole-dipole attraction and the external force change. These structures, formed from four or more particles, resemble those studied in [7, 8]. By performing simulations over a wide range of parameter values, we identify the conditions for observing different dynamic regimes in the system: a stationary kink, a running kink, a cluster kink, and chain drift.

FUNDING

A.E.S. acknowledges the support from the Russian Science Foundation under Project no. 23-12-00180.

CONFLICT OF INTEREST

The authors of this work declare that they have no conflicts of interest.

REFERENCES

1. Xiao, Z., Wie, M., and Wang, W., *ACS Appl. Mater. Interfaces*, 2019, vol. 11, no. 7, p. 6667.
2. Alapan, Y., Bozuyuk, U., Erkoc, P., et al., *Sci. Rob.*, 2020, vol. 5, no. 42, p. eaba5726.
3. Braun, O.M. and Naumovets, A.G., *Surf. Sci. Rep.*, 2006, vol. 60, nos. 6–7, p. 79.
4. Vanossi, A., Bechinger, C., and Urbakh, M., *Nat. Commun.*, 2020, vol. 11, p. 4657.
5. Bohlein, T., Mikhael, J., and Bechinger, C., *Nat. Mater.*, 2012, vol. 11, p. 126.
6. Juniper, M.P.N., Straube, A.V., Besseling, R., et al., *Nat. Commun.*, 2015, vol. 6, p. 7187.
7. Antonov, A.P., Ryabov, A., and Maass, P., *Phys. Rev. Lett.*, 2022, vol. 129, no. 8, p. 080601.
8. Cereceda-López, E., Antonov, A.P., Ryabov, A., et al., *Nat. Commun.*, 2023, vol. 14, p. 6448.
9. Juniper, M.P.N., Straube, A.V., Aarts, D.G.A.L., et al., *Phys. Rev. E*, 2016, vol. 93, no. 1, p. 012608.
10. Juniper, M.P.N., Besseling, R., Aarts, D.G.A.L., and Dullens, R.P.A., *Opt. Express*, 2012, vol. 20, no. 12, p. 28707.

11. Stoop, R.L., Straube, A.V., and Tierno, P., *Nano Lett.*, 2019, vol. 19, no. 1, p. 433.
12. Adler, R., *Proc. IRE*, 1946, vol. 34, no. 6, p. 351.
13. Carstensen, H., Kapaklis, V., and Wolff, M., *Phys. Rev. E*, 2015, vol. 92, no. 1, p. 012303.
14. Ivanov, A.O. and Subbotin, I.M., *Bull. Russ. Acad. Sci.: Phys.*, 2024, vol. 88, no. 10, p. 1579.
15. Anderson, R.A. and Martin, J.E., *Am. J. Phys.*, 2002, vol. 70, no. 12, p. 1194.
16. Bondar', E.V., Shel'deshova, E.V., Shabanova, I.A., and Ryapolov, P.A., *Bull. Russ. Acad. Sci.: Phys.*, 2024, vol. 88, no. 10, p. 1648.
17. Straube, A.V. and Tierno, P., *Soft Matter*, 2014, vol. 10, no. 22, p. 3915.
18. Weeks, J.D., Chandler, D., and Andersen, H.C., *J. Chem. Phys.*, 1971, vol. 54, no. 12, p. 5237.
19. Cereceda-López, E., Ostinato, M., Ortiz-Ambriz, A., et al., *Phys. Rev. Res.*, 2024, vol. 6, no. 1, p. L012044.
20. Straube, A.V., Dullens, R.P.A., Schimansky-Geier, L., and Louis, A.A., *J. Chem. Phys.*, 2013, vol. 139, no. 13, p. 134908.